Graefe's Archive for Clinical and Experimental Ophthalmology (2019) 257:1915–1924
https://doi.org/10.1007/s00417-019-04422-y

BASIC SCIENCE

Mesenchymal cells and fluid flow stimulation synergistically regulate the kinetics of corneal epithelial cells at the air–liquid interface

Kosuke Kawata[1,2] · Shigehisa Aoki[1] · Maki Futamata[1] · Mihoko Yamamoto-Rikitake[1] · Isao Nakao[2] · Hiroshi Enaida[2] · Shuji Toda[1]

Received: 22 March 2019 / Revised: 20 June 2019 / Accepted: 10 July 2019 / Published online: 18 July 2019
© Springer-Verlag GmbH Germany, part of Springer Nature 2019

Abstract

Purpose In vivo microenvironments are critical to tissue homeostasis and wound healing, and the cornea is regulated by a specific microenvironment complex that consists of cell–cell interactions, air–liquid interfaces, and fluid flow stimulation. In this study, we aimed to clarify the effects of and the correlations among these three component factors on the cell kinetics of corneal epithelial cells.

Methods Human corneal epithelial–transformed (HCE–T) cells were cocultured with either primary rat corneal fibroblasts or NIH 3T3 fibroblasts. We employed a double-dish culture method to create an air–liquid interface and a gyratory shaker to create fluid flow stimulation. Morphometric and protein expression analyses were performed for the HCE–T cells.

Results Both the primary rat fibroblasts and the NIH 3T3 cells promoted HCE–T cell proliferation, and the presence of fluid flow synergistically enhanced this effect and inhibited the apoptosis of HCE–T cells. Moreover, fluid flow enhanced the emergence of myofibroblasts when cocultured with primary rat fibroblasts or NIH 3T3 cells. Extracellular signal-regulated kinase and p38 signaling were regulated either synergistically or independently by both fluid flow and cellular interaction between the HCE–T and NIH 3T3 cells.

Conclusion The cell–cell interaction and fluid flow stimulation in the air–liquid interface synergistically or independently regulated the behavior of HCE–T cells. Fluid flow accelerated the phenotypic change from corneal fibroblasts and NIH 3T3 cells to myofibroblasts. Elucidation of the multicomponent interplay in this microenvironment will be critical to the homeostasis and regeneration of the cornea and other ocular tissues.

Keywords Corneal microenvironment · Shear stress · Cell–cell interaction · Wound healing

Introduction

The cornea is a transparent tissue and is composed of five layers: the multilayered corneal epithelium, Bowman's membrane, the corneal stroma, Descemet's membrane, and the corneal endothelial layer (Fig. 1a) [1]. Both corneal epithelial cells and stromal keratocytes possess the paracrine loop and regulate the homeostasis and wound healing process of the cornea [2]. The cornea exists in the air–liquid interface, which is composed of lacrima (the covering watery fluid) and the surrounding atmosphere [3]. In addition, corneal stromal cells are exposed to interstitial fluid flow produced by the aqueous humor from the anterior chamber [4].

In vivo microenvironments are critical for tissue homeostasis and the wound healing process [5, 6]. The paracrine loop that originates during cell–cell interaction is a cellular factor of the microenvironment [7]. Physical stimulation such as fluid shear is in turn a location-specific factor of the microenvironment of a given tissue [8]. In cornea, lacrima is stirred by palpebration and eye movement, and corneal epithelial cells are constantly exposed to fluid flow stimulation. In addition, these corneal epithelial cells are in the air–liquid interface composed of lacrima and air at the surface of the eye. We hypothesized that there may be a connection, in the cornea, among interactions between epithelial and stromal cells, fluid flow stimulation, and the air–liquid interface and that each of these three factors may

✉ Shigehisa Aoki
aokis@cc.saga-u.ac.jp

[1] Department of Pathology and Microbiology, Faculty of Medicine, Saga University, 5–1–1 Nabeshima, Saga 849–8501, Japan

[2] Department of Ophthalmology, Faculty of Medicine, Saga University, Saga, Japan

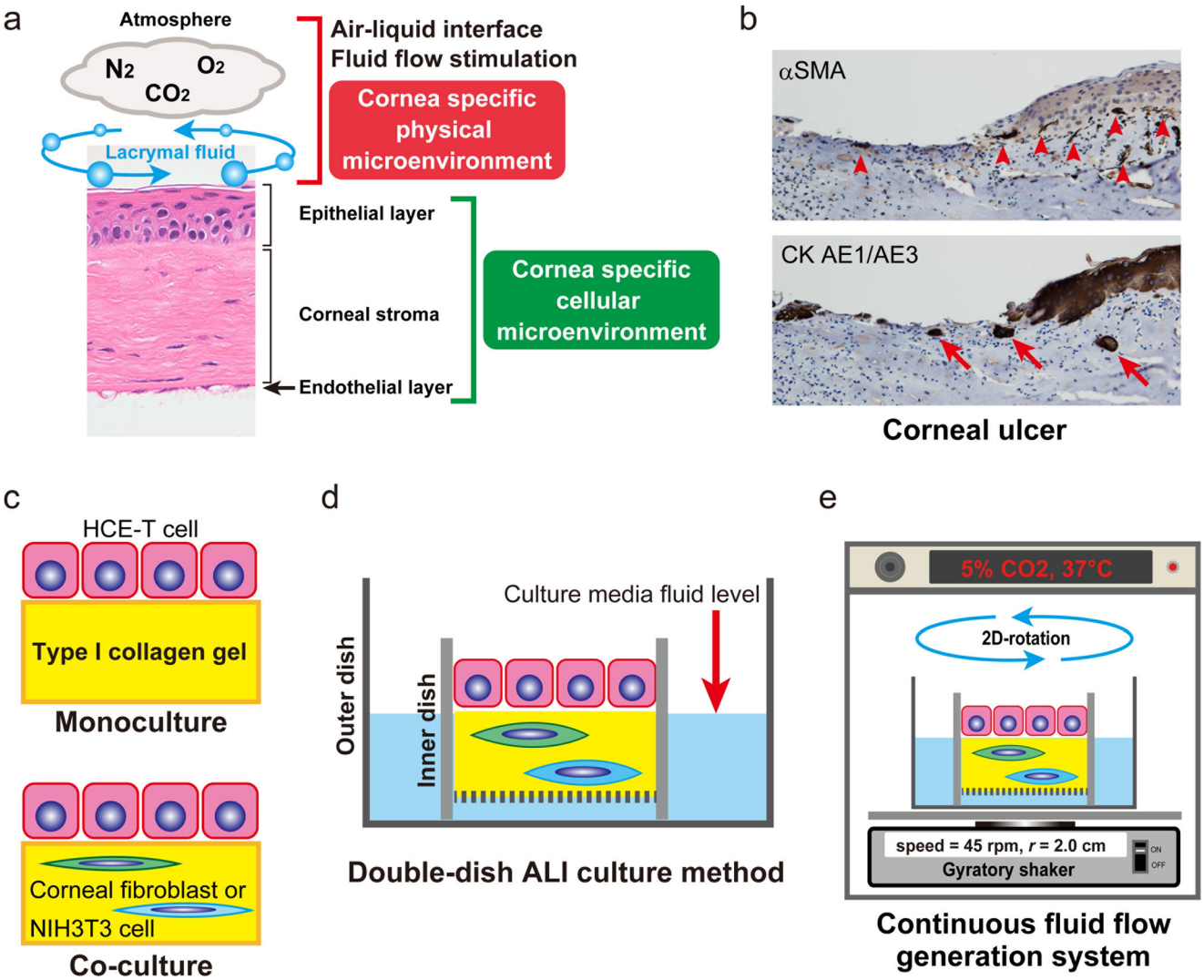

Fig. 1 Corneal microenvironment and experimental design. **a** Corneal physical and cellular microenvironment. The cornea exists with an air–liquid interface composed of the covering watery lacrimal fluid and the surrounding air. The cornea itself consists of three cellular layers: the epithelial layer, the corneal stroma, and the endothelial layer. The interaction between the epithelial and stromal layers constitutes a specific cellular microenvironment of the cornea. **b** Histologic features of corneal ulcers. In this illustration, alpha-smooth muscle actin (αSMA)–positive myofibroblasts are located beneath the epithelial layer and the surface of the eroded corneal stroma (arrowhead). Cytokeratin (CK) AE1/AE3 immunostaining shows epithelial cell invagination into the corneal stroma (arrow). **c** Coculture models of human corneal epithelium–transformed (HCE–T) cells seeded on collagen gel discs embedded with corneal fibroblasts or NIH 3T3 cells. As a control, HCE–T cells were seeded on collagen gel discs without stromal cells. **d** Double-dish air–liquid interface (ALI) culture method. To replicate the air–liquid interface, the culture fluid level of outer dish was adjusted to the height of collagen gel of the inner dish. **e** Continuous fluid flow–generating system. To generate fluid flow, culture dishes were placed on a gyratory shaker in a CO_2 incubator

have an important role to play in the homeostasis of corneal tissue as a specific constituent of the microenvironment. No culture models that can simultaneously reconstruct cell–cell interaction, fluid flow stimulation, and air–liquid interface are available. To the best of our knowledge, we overcame this issue by establishing a simple culture model that could concurrently replicate the cellular and physical microenvironments in the cornea.

This study aimed to clarify the effect of both the cellular and physical microenvironments on the homeostasis and wound healing in corneal tissue.

Methods

Cell lines and tissue samples

Human corneal epithelial–transformed (HCE–T) cell lines were obtained from the RIKEN Cell Bank (Ibaraki, Japan) and maintained in Roswell Park Memorial Institute (RPMI) 1640 medium supplemented with 10% fetal bovine serum (FBS), 0.5% dimethyl sulfoxide, 100 μ/mL streptomycin, and 100 μ/mL penicillin. NIH 3T3 mouse fibroblasts were obtained from the Japanese Cancer

Research Bank, Osaka. NIH 3T3 cell lines were maintained in RPMI 1640 medium supplemented with 10% FBS, 100 μ/mL streptomycin, and 100 μ/mL penicillin. Primary corneal fibroblasts were isolated from the corneal tissue of 4- to 6-week-old Wistar rats. To isolate cells, the corneas were incubated in a 3-mg/mL collagenase A solution for 1 h at 37 °C with a stirring device. The digest was then immediately placed in a monolayer culture and maintained in RPMI 1640 medium supplemented with 10% FBS, 100 μ/mL streptomycin, and 100 μ/mL penicillin. Under the culture condition, isolated keratocytes lost their phenotype and differentiated into fibroblasts in the presence of FBS [9]. All cell lines were incubated in a humidified atmosphere of 5% CO_2 and 20% O_2 at 37 °C in a CO_2 incubator.

Air–liquid interface cell culture system

To analyze the cell–cell interaction and kinetics of HCE–T cells, we developed a double-dish culture system (Fig. 1c) [10, 11]. First, corneal fibroblasts or NIH 3T3 cells were mixed with a collagen gel solution (Cellmatrix, type I-A; Nitta Gelatin Co. Ltd., Osaka). Next, 1 mL of the mixture (including 5×10^5 keratocytes or NIH 3T3 cells) was poured into 30-mm-diameter Millicell-CM dishes (Millipore, Bedford, Massachusetts, USA). After the gel was solidified at 37 °C for 30 min, 2×10^5 HCE–T cells were seeded onto the surface of each dish. These dishes were then placed in larger (90-mm-diameter) outer dishes (Sumitomo Bakelite, Japan) containing 9 mL of complete medium in an air–liquid interface condition (Fig. 1d). To serve as controls, HCE–T cells were also seeded on collagen gel dishes without mesenchymal cells. Primary corneal keratocyte cells isolated from the corneal tissue of Wistar rats were cocultured with HCE–T, as previously described.

Fluid flow–generating system

The fluid flow–generating system was slightly modified from a method used previously [12]. One day after HCE–T cells were seeded, dishes were incubated in a system that generated fluid flow. The culture dishes were incubated in an atmosphere of 5% CO_2 and 20% O_2 at 37 °C in a CO_2 incubator; to generate flow, the dishes were placed on a gyratory shaker (MIR–S100C; Panasonic, Tokyo, Japan) that rotated at a speed of 45 rpm (Fig. 1e). Control dishes were placed in the CO_2 incubator when static, and the culture medium was changed every other day. In this way, the HCE–T cells were exposed to both an air–liquid interface and a fluid flow condition, which mimicked the in vivo physical microenvironment of the cornea.

Histology and immunohistochemistry

After 14 days of culturing, we performed histological examinations with hematoxylin–eosin staining. Tissues were fixed with 10% formalin, routinely processed, and embedded in paraffin, before deparaffinized sections were used for staining. A mouse monoclonal anti-pan–cytokeratin (CK) AE1/AE3 antibody was used to detect HCE–T cells, and a mouse monoclonal alpha-smooth muscle actin (αSMA) antibody (Dako, Glostrup, Denmark) was used to evaluate the myofibroblasts. Proliferative and apoptotic cells were labeled with a mouse monoclonal anti-Ki-67 antibody (Dako) and a rabbit monoclonal cleaved caspase-3 antibody (Cell Signaling Technology, Danvers, Massachusetts), respectively. For immunofluorescence analyses, a rabbit monoclonal anti-αSMA antibody conjugated with Alexa Fluor 488 was used. Alexa Fluor 568-conjugated goat anti-mouse immunoglobulin G (Invitrogen, Carlsbad, CA) was used as the antibody secondary to CK AE1/AE3 antibody. Images were analyzed with an Axio Imager 2 light microscope and Apotome.2 system (Carl Zeiss Co. Ltd., Oberkochen, Germany).

Morphometric analysis

A total of 1000 cells were counted (low magnification, × 10 objective) at five randomly chosen noncontiguous and nonoverlapping fields of the stained sections. The percentages of Ki-67-positive cells and cleaved caspase-3–positive cells were then determined as indicators of proliferation and apoptosis, respectively. The epithelial cell layer thickness was measured at ten points in the five randomly chosen areas. The depth of HCE–T cell invagination was measured from the basement membrane to the deepest part of the HCE–T cells.

Western blot analysis

Experiments were performed with the samples in submerged conditions for the protein analysis. HCE–T cells and NIH 3T3 cells were cocultured in inserts with 8-μm pore sizes (Falcon Cell Culture Insert; Becton Dickinson, Franklin Lakes, N.J.). NIH 3T3 cells embedded in collagen gels were placed on the outside bottom of the inserts, and HCE–T cells were seeded inside the inserts. The inserts were then placed in 10-cm-diameter dishes in 20 mL of complete medium and were adjusted to the air–liquid interface condition. After culturing for 48 h, the collagen gels were stripped from the inserts. The HCE–T cells were lysed in 400 μL of M-PER Reagent (ThermoFisher Scientific, Waltham, Massachusetts) containing Protease/Phosphatase Inhibitor Cocktail (Cell Signaling Technology). Lysates containing an equal quantity of protein were separated by sodium dodecyl sulfate–polyacrylamide gel electrophoresis in 12% bis-tris gels and transferred to polyvinylidene difluoride membranes. The membranes were

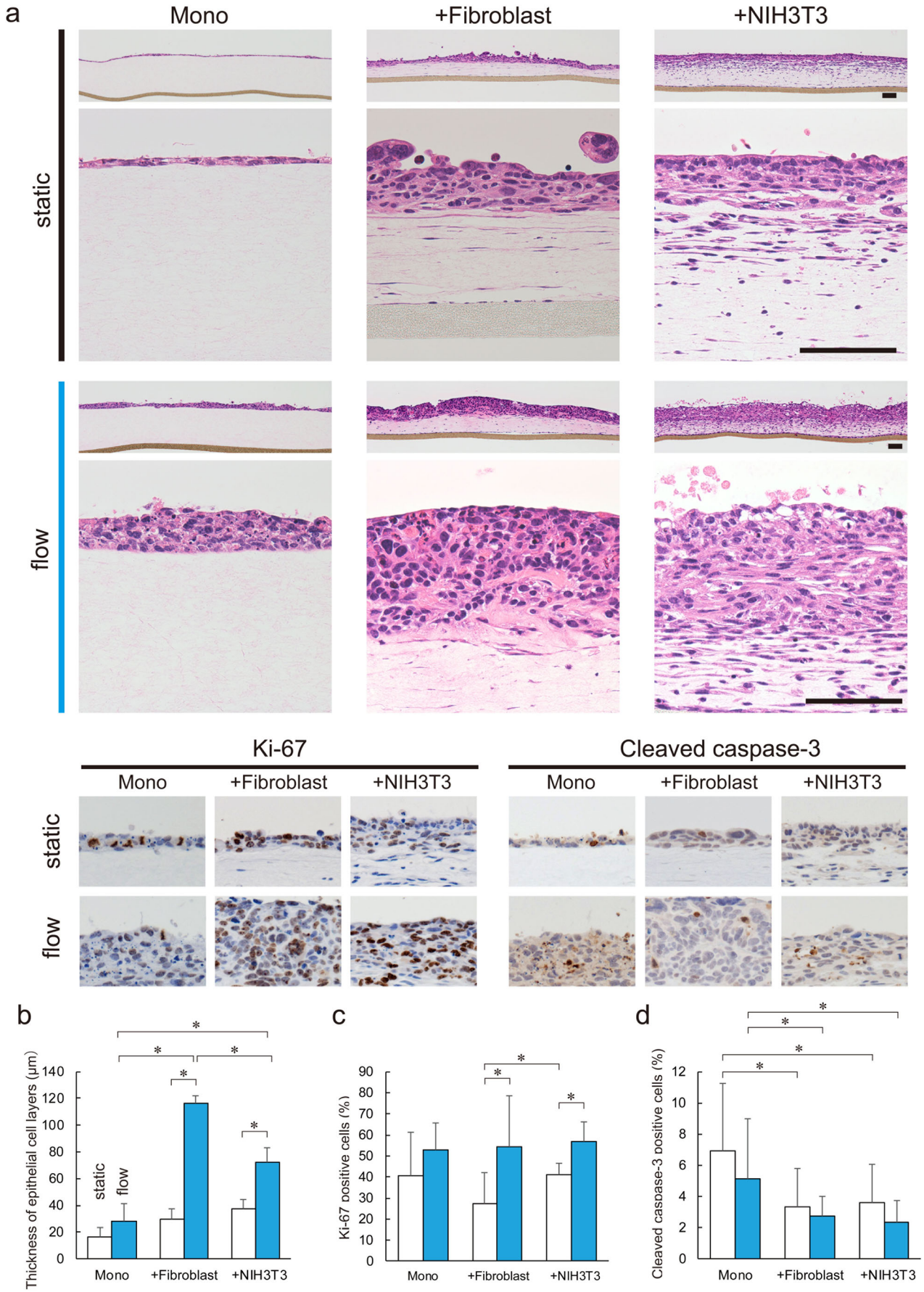
a
Mono
+Fibroblast
+NIH3T3
static
flow
Ki-67
Cleaved caspase-3
b
Thickness of epithelial cell layers (μm)
c
Ki-67 positive cells (%)
d
Cleaved caspase-3 positive cells (%)

◀ **Fig. 2** Effects of stromal cells and fluid flow on the cellular kinetics of HCE–T cells. **a** At day 14, both keratocyte and NIH 3T3 cells synergistically promoted cellular hypertrophy and thickened epithelium layer in HCE–T cells in conditions of fluid flow. HCE–T cells cultured with fibroblasts and NIH 3T3 cells invaded the corneal stroma. Upper and lower pictures show low and high magnification images, respectively. Abbreviation: Mono, monoculture. Bar, 100 μm. **b** Immunostaining of Ki-67 ad cleaved caspase-3. **c** Thickness of epithelial cell layers. **d** Immunostaining for Ki-67 and the percentages of positive cells. **e** Immunostaining for cleaved caspase-3 and percentages of positive cells. Data are shown as means ± standard deviation of the mean for three measures. *$p < 0.05$. White and blue bar charts indicate the static and fluid flow conditions, respectively

incubated overnight at 4 °C with antibodies against extracellular signal–regulated kinase (ERK) 1/2, p-ERK1/2, p38, and p-p38 (Cell Signaling Technology). A chemiluminescent immunodetection system (Western Breeze; ThermoFisher Scientific) was used to detect antibody-bound antigens on membranes. Band densities were determined using a Fusion system (Vilber–Lourmat, Eberhardzell, Germany), analyzed with Image J software (http://rsb.info.nih.gov/ij/), and presented as ratios relative to control values.

Statistical analysis

Data obtained from three to five independent experiments were analyzed with Student's *t* tests or Wilcoxon tests, depending on the results of equality of variance. Values are presented as means ± standard deviations, together with the number of experiments carried out. Mean values of replicates in experiments were used to determine statistical significance; *p* values of less than 0.05 indicated statistically significant differences. All statistical analyses were performed using JMP 13 for Windows (SAS, Cary, N.C.).

Results

Synergism of mesenchymal cells and fluid flow in HCE–T cells at the air–liquid interface

Because the air–liquid interface is an essential microenvironment for corneal cell culture [10, 11], all experiments were performed in this condition.

To clarify mesenchymal paracrine and fluid flow stimulation effects, we cultured HCE–T cells with primary corneal fibroblasts derived from rat corneal tissue or NIH 3T3 fibroblasts in the static and fluid flow conditions, as mentioned previously. The HCE–T cells cultured without mesenchymal cells showed a flat cytoplasm with a one- to two-layer structure in the static conditions (Fig. 2a). When they were cultured with primary keratocytes, however, cellular hypertrophy was induced, and the thickness of the HCE–T cell layer increased. When they were cultured with NIH 3T3 cells in the static conditions, there was mild cytoplasmic hypertrophy with increased sheet-like thickness of cells. Both fibroblasts and NIH 3T3 cells triggered HCE–T cell invagination into the collagen gel layer, which was not present in the monoculture group, in both static and fluid flow conditions.

Next, we added fluid flow stimulation to the cell cultures to investigate the role of the physical microenvironment. HCE–T cells in the monoculture group showed cytoplasmic hypertrophy and a thickened cellular layer in conditions of fluid flow stimulation (Fig. 2a). The presence of fibroblasts or NIH 3T3 cells also induced greater cell numbers, a greater ratio of nuclear cells to cytoplasmic cells, and an increase in multistratified layers in HCE–T cells. The respective thicknesses of cellular layers in the groups in the static and fluid flow conditions were 16.3 ± 7.1 μm and 28.0 ± 13.3 μm, respectively, for HCE–T monocultures; 29.7 ± 7.9 μm and 116.8 ± 5.1 μm, respectively, for HCE–T cells plus fibroblasts; and 37.4 ± 7.3 μm and 72.6 ± 10.3 μm, respectively, for HCE–T cells plus NIH 3T3 cells.

In static conditions, there was a difference between the groups cocultured with fibroblasts and those cocultured with NIH 3T3. Fluid flow significantly increased the ratio of Ki-67-positive HCE–T cells cocultured with either fibroblasts or NIH 3T3 cells, in comparison with these groups in static conditions. The respective Ki-67 labeling index percentages in the groups in static and fluid flow conditions were 40.7% ± 20.7% and 52.9% ± 12.6%, respectively, for HCE–T monocultures; 27.5% ± 14.4% and 54.6% ± 24.1%, respectively, for HCE–T cells plus fibroblasts; and 41.2% ± 5.2% and 56.7% ± 9.8%, respectively, for HCE–T cells plus NIH 3 T3 cells (Fig. 2c).

Fibroblasts and NIH 3T3 cells had a lower labeling index of HCE–T cells positive for cleaved caspase-3 than did the monoculture group in static and fluid flow conditions (Fig. 2d). Fluid flow did not affect the cleaved caspase-3 labeling index in any group. The respective percentages for the cleaved caspase-3 labeling indexes in the groups in static and fluid flow conditions were 6.9% ± 4.3% and 5.1% ± 3.8%, respectively, for HCE–T monocultures; 3.4% ± 2.4% and 2.7% ± 1.2%, respectively, for HCE–T cells plus fibroblasts; and 3.6% ± 2.5% and 2.3% ± 1.4%, respectively, for HCE–T cells plus NIH 3T3 cells.

Mesenchymal cells and fluid flow promote HCE–T cell invagination into collagen matrix at the air–liquid interface

Corneal damage induces keratocytes to differentiate into myofibroblasts [13]. These then regulate the deposition and organization of extracellular matrix in corneal wounds and are responsible for corneal wound contraction [14], and both the epithelial–mesenchymal transition of epithelial cells and the activated stromal niche regulate

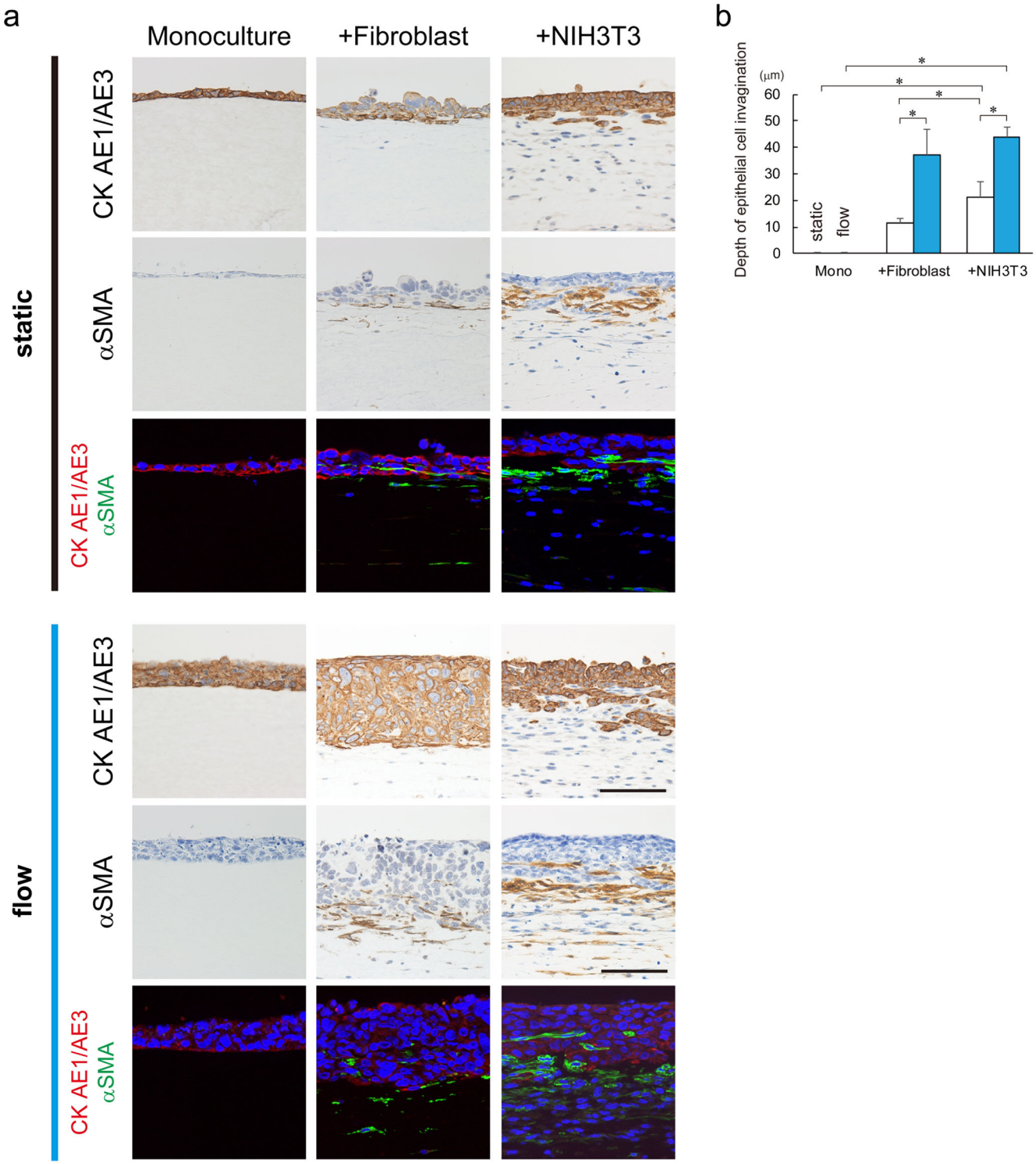

Fig. 3 Stromal cells and fluid flow promote frequent myofibroblast emergence and HCE–T cell invagination **a** Myofibroblasts emerged beneath the epithelial layer in the group cocultured with fibroblasts or NIH 3T3 cells in the static condition. NIH 3T3 cells promoted more frequent myofibroblast emergence compared with the fibroblasts. Fibroblasts and NIH 3T3 cells induced HCE–T cells to invaginate into the collagen gel. Fluid flow enhanced this invagination of HCE–T cells. Immunofluorescence images of border area of epithelial cell layers and mesenchymal cells (green, αSMA; red, cytokeratin [CK] AE1/AE3; blue, DAPI). αSMA and cytokeratin AE1/AE3 double–positive cell is difficult to detect. **b** Depth of epithelial cell invagination area. Data are shown as means ± standard deviation of the mean for three measures. Bar, 100 μm. *$p < 0.05$. White and blue bar chart indicates the static and fluid flow conditions, respectively. Abbreviations: Mono, monoculture; αSMA, alpha-smooth muscle actin

intrastromal invasion of limbal epithelial cells [15]. Any disarrangement of corneal epithelial cells and keratocytes then induces corneal opacity [16].

The monoculture group had no αSMA-positive cells in the static or fluid flow conditions, but αSMA-positive myofibroblasts emerged beneath the HCE–T cells in the groups cocultured with fibroblasts or NIH 3T3 cells in the static conditions (Fig. 3a). The frequency of myofibroblast emergence was higher in the group cocultured with NIH 3T3 than in the group cocultured with fibroblasts. Away from the epidermal layer, neither fibroblasts nor NIH 3T3 cells showed αSMA-positive phonotypes. Compared with the static condition, fluid flow increased the number of myofibroblasts in the affected area in both the keratocyte and the NIH 3T3 coculture groups. Compared with the static condition, fluid flow also increased the distributed range and depth of myofibroblasts from fibroblasts and NIH 3T3 cells in the affected area. Myofibroblasts emerged inside the thickened epithelial layers cocultured with fibroblasts and NIH3T3 cells under fluid flow condition, but the CK AE1/AE3 and αSMA double-positive cell was not observed. During corneal regeneration, corneal epithelial cells often invaginate into the stroma in the manner of rete ridges of the skin [17]. To assess this, we measured the invagination depths of HCE–T cells into collagen gel. In the absence of mesenchymal cells, HCE–T cells did not invaginate into collagen gel in either the static or fluid flow condition. In contrast, the presence of fibroblasts and NIH 3T3 cells induced invagination, and this was promoted by fluid flow. The respective depths of invagination in groups in the static and fluid flow conditions were 0 μm and 0 μm, respectively, for HCE–T monocultures; 11.6 ± 1.7 μm and 37.0 ± 9.9 μm, respectively, for HCE–T cells plus fibroblasts; and 21.0 ± 6.0 μm and 43.9 ± 3.9 μm, respectively, for HCE–T cells plus NIH 3T3 cells.

Fibroblasts and fluid flow modulate ERK1/2 and p38 expression in HCE–T cells

Mitogen-activated protein kinase (MAPK) pathways are involved in the proliferation, epithelial–mesenchymal transition, and migration of many cell types, including those of the cornea [18]. To achieve reproducible results, we used NIH 3T3 cells as the representative mesenchymal cell, and we evaluated ERK1/2 and p38 expression to clarify the kinetics of HCE–T cells.

The total ERK expression of HCE–T cells did not differ significantly between the monoculture and NIH 3T3 cocultured groups in the static or fluid flow conditions (Fig. 4). Fluid flow caused significant downregulation of the total ERK expression in the monoculture group, in comparison with the static condition. There was no difference in the ratios of phosphorylated ERK1/2 to total ERK1/2 in the monoculture group in the static and fluid flow conditions. In comparison with the static condition, fluid flow caused significant upregulation of the ratio of phosphorylated ERK1/2 to total ERK1/2 in the monoculture group, in comparison with the NIH 3T3 coculture group.

There was no significant difference in total p38 expression of HCE–T cells between the monoculture and NIH 3T3 coculture groups in the static or fluid flow conditions. The ratio of phosphorylated p38 to total p38 was significantly lower in the monoculture group than that in the NIH 3T3 coculture group in the static condition. Fluid flow caused upregulation of the ratio of phosphorylated p38 to total p38 in the monoculture group in comparison with the static condition but caused downregulation of that ratio in the NIH 3T3 coculture group.

Discussion

In this study, we demonstrated that three microenvironments—interaction between cells, stimulation by fluid flow, and the presence of an air–liquid interface—synergistically regulated the behavior of corneal epithelial cells. We assessed this synergy by using a new three-dimensional culture system.

Physical stress, especially fluid flow, has been implicated in the physiologic response to endothelial cells [19, 20]. Shear stress and fluid flow constitute critical microenvironmental factors in various cell types, including stem cells and cancer cells [21, 22]. In the eye, corneal epithelial cells and stromal cells are surrounded continuously by lacrimal and aqueous humor, respectively. These two fluids are involved in fluid flow during blinking, eye movement, and aqueous outflow. Several researchers have reported that the cell kinetics of corneal epithelial cells or endothelial cells are individually affected by the resulting shear stress [23–27]. However, these researchers used only two-dimensional, single-cell culture models and did not consider the air–liquid interfaces that are key for organs covering or covered by the body (e.g., eyes, skin, and gastrointestinal tract). According to previous reports, reconstructing this particular physical environment in a culture model affected cellular proliferation, apoptosis, differentiation, and stemness in several normal and cancer tissues [10, 28–30]. It is therefore essential that investigators replicate the tissue architecture, cell–cell interactions, and specific physical microenvironment in a three-dimensional culture system that in order to interpret cell kinetics and remodeling accurately.

Cell–cell interaction is critical for maintaining tissue homeostasis and regeneration of both normal and cancer tissue [31, 32], and a mesenchymal paracrine effect is attributed to cell–cell interaction and exerts proliferative, anti-apoptotic, and anti-inflammatory effects to parenchymal cells [33, 34]. Our culture model also replicated the anti-apoptotic paracrine effect of fibroblasts and NIH 3T3 cells in corneal epithelial cells independently of fluid flow stimulation. In contrast, the

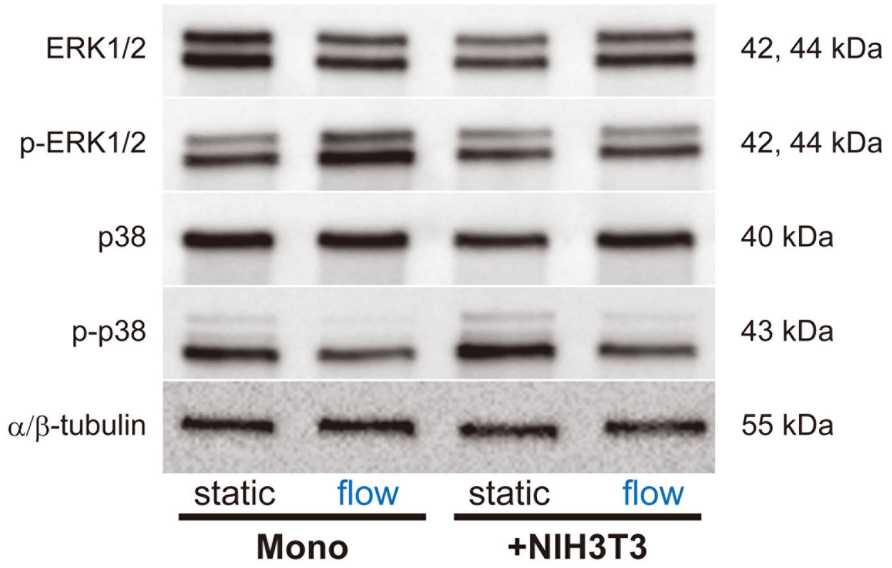
ERK1/2
42, 44 kDa
p-ERK1/2
42, 44 kDa
p38
40 kDa
p-p38
43 kDa
α/β-tubulin
55 kDa
static
flow
static
flow
Mono
+NIH3T3

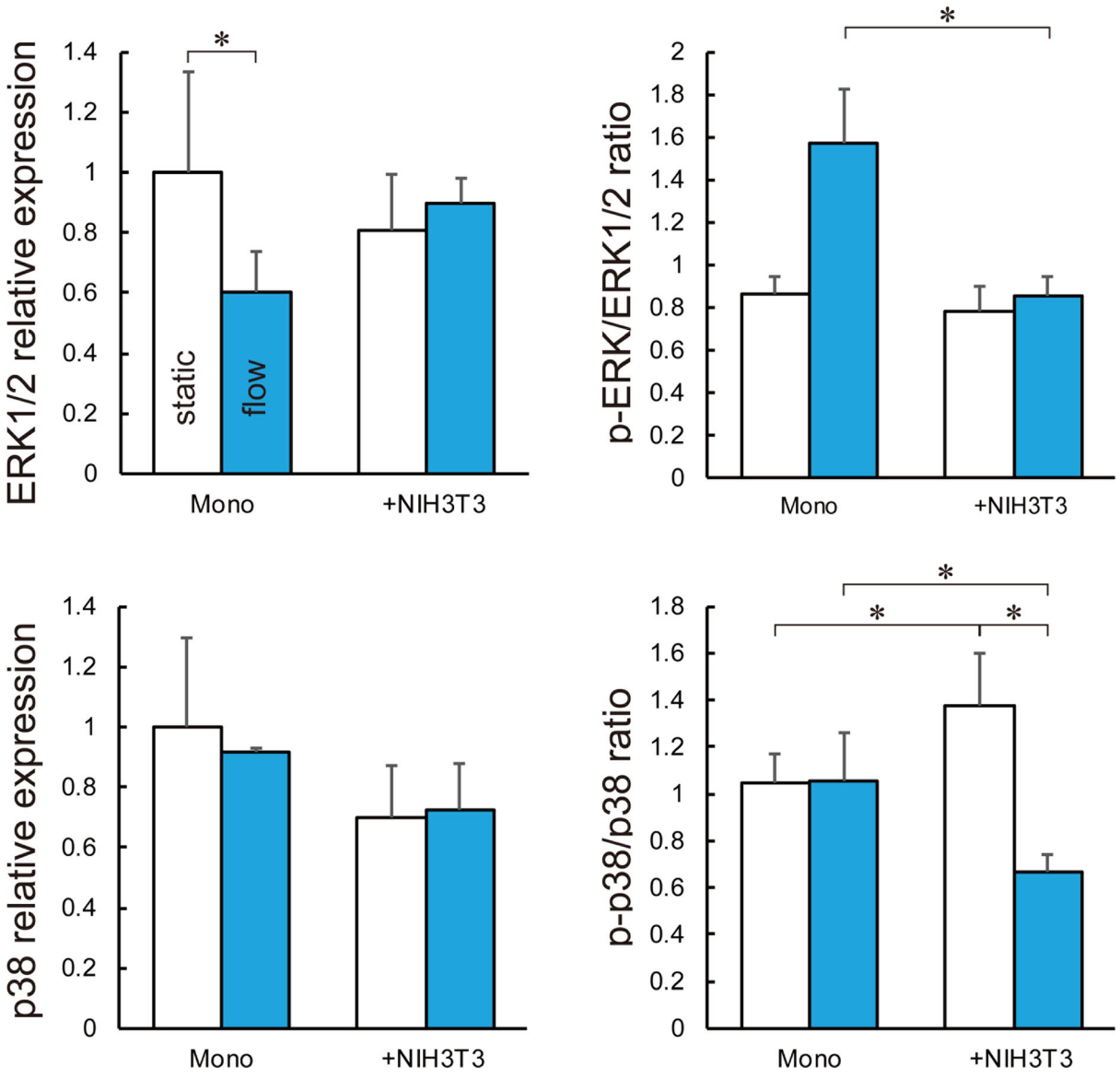
ERK1/2 relative expression
p-ERK/ERK1/2 ratio
p38 relative expression
p-p38/p38 ratio
static
flow
Mono
+NIH3T3
*

◀ **Fig. 4** Effect of NIH 3T3 cells and fluid flow on mitogen-activated protein kinase (MAPK) expression in HCE–T cells. Protein expression levels in HCE–T cells were evaluated with Western blot. Relative expression is depicted as the ratio of target protein expression to α- and β-tubulin expression. Data are presented as means ± standard deviations of 3–5 determinations. $*p < 0.05$. White and blue bar charts indicate the static and fluid flow conditions, respectively. Abbreviations: ERK1/2, extracellular signal-regulated kinases 1 and 2; p-, phosphor-; Mono, monoculture

effect of physical stimulation on cell–cell interactions is not fully understood. In this study, we demonstrated that a phenotypic change from keratocyte or fibroblast to myofibroblast was promoted by fluid flow stimulation in the air–liquid interface. Moreover, MAPK signaling was synergistically or independently regulated by the interaction between cells and the stimulation by fluid flow. Our simple culture model helped us determine the factors that affected the behavior of corneal epithelial cells in order to evaluate the kinetics of corneal cells in a manner consistent with the in vivo environment.

Corneal ulceration can be highly detrimental to visual acuity, potentially causing loss of vision in the most severe cases [35]. Such ulcers have been attributed to the loss and deformation of the extracellular matrix material of corneal tissue. Several researchers have also reported that injury-induced activation and phenotypic transformation from fibroblasts to myofibroblasts regulate the deposition and organization of extracellular matrix in corneal wounds [14, 36]. Myofibroblasts play a central role in the control of an interconnected meshwork of cells and extracellular matrix that deposits regenerative matrix and contracts corneal wounds [37]. In addition, epithelial–mesenchymal transition is recognized to occur in a limbal site in cases of corneal injury and is involved in the fibrotic process of corneal regeneration. Pathological fibrotic and re-epithelizing processes cause vision-threatening diseases such as severe ocular surface fibrosis [38]. Although the importance of myofibroblasts is widely recognized, no suitable application for in vitro analysis was previously established. In this study, we proposed that replication of both corneal cell–cell interaction and the specific microenvironment is essential for understanding the corneal wound healing process.

The activation of MAPK signaling is a key factor in the transition of fibroblasts to myofibroblasts [39, 40]. However, our data showed that with fluid flow stimulation, the number of myofibroblasts increased and phosphorylation of ERK and p38 of HCE–T cells cocultured with NIH 3T3 cells decreased. We previously demonstrated that fluid flow stimulation promoted peritoneal fibrosis via epithelial–mesenchymal transition of mesothelial cells [12]. In addition, fluid flow stimulation inhibited both the total expression and phosphorylation ratio of ERK1/2 and p38 of mesothelial cells, and ERK and p38 inhibitors replicated the fibrotic change caused by mesothelial cells without fluid flow stimulation in the same manner. Fluid flow stimulation may regulate non-ERK or non-p38 signaling, and the signaling of an unknown entity may increase the emergence of myofibroblasts and inhibit the expression of ERK and p38.

In conclusion, we established a reconstruction model for concurrently investigating the cellular and physical microenvironments of corneal tissue. This alternative culture model is a promising tool to aid with further therapeutic investigation into cornea-damaging disease.

Acknowledgments We are grateful to Professor S. Aishima and Dr. M. Hashiguchi for useful discussion and for sharing their dataset, and we thank T. Sakumoto, S. Morito, M. Nishida, F. Mutoh, S. Nakahara, and I. Nanbu for their excellent technical assistance. We also thank Mr. K. Tokaichi for refining the English of the manuscript. We also thank Enago (www.enago.jp) for the English language review.

Funding This work was supported in part by the Center for Clinical and Translational Research of Kyushu University Hospital (to S.A.), and Grants-in-Aid from the Japanese Ministry of Education, Culture, Sports, Science and Technology for Scientific Research (no. 16K09284 to S.A. and no. 18K09451 to H.E.).

Compliance with ethical standards

All animal experiments complied with the guidelines of the Association for Research in Vision and Ophthalmology (ARVO) Statement for the Use of Animals in Ophthalmic and Vision Research.

Conflict of interest The authors declare that they have no conflict of interest.

Ethical approval All applicable international, national, and institutional guidelines for the care and use of animals were followed.

References

1. Pawlina W, Ross MH (2018) Histology: a text and atlas: with correlated cell and molecular biology. Wolters Kluwer Health, Philadelphia
2. Wilson SE, Mohan RR, Mohan RR, Ambrosio R Jr, Hong J, Lee J (2001) The corneal wound healing response:: cytokine-mediated interaction of the epithelium, stroma, and inflammatory cells. Prog Retin Eye Res 20(5):625–637
3. Zhang X, Vimalin Jeyalatha M, Qu Y, He X, Ou S, Bu J, Jia C, Wang J, Wu H, Liu Z, Li W (2017) Dry eye management: targeting the ocular surface microenvironment. Int J Mol Sci 18(7). https://doi.org/10.3390/ijms18071398
4. Joyce N (2003) Proliferative capacity of the corneal endothelium. Prog Retin Eye Res 22(3):359–389. https://doi.org/10.1016/s1350-9462(02)00065-4
5. Blanpain C, Fuchs E (2009) Epidermal homeostasis: a balancing act of stem cells in the skin. Nat Rev Mol Cell Biol 10(3):207
6. Diegelmann RF, Evans MC (2004) Wound healing: an overview of acute, fibrotic and delayed healing. Front Biosci 9(1):283–289
7. Joyce JA, Pollard JW (2009) Microenvironmental regulation of metastasis. Nat Rev Cancer 9(4):239
8. Walker GM, Zeringue HC, Beebe DJ (2004) Microenvironment design considerations for cellular scale studies. Lab Chip 4(2):91–97

9. Fernandez-Perez J, Ahearne M (2019) Influence of biochemical cues in human corneal stromal cell phenotype. Curr Eye Res 44(2):135–146. https://doi.org/10.1080/02713683.2018.1536216
10. Minami Y, Sugihara H, Oono S (1993) Reconstruction of cornea in three-dimensional collagen gel matrix culture. Invest Ophthalmol Vis Sci 34(7):2316–2324
11. Nishimura T, Toda S, Mitsumoto T, Oono S, Sugihara H (1998) Effects of hepatocyte growth factor, transforming growth factor-beta1 and epidermal growth factor on bovine corneal epithelial cells under epithelial-keratocyte interaction in reconstruction culture. Exp Eye Res 66(1):105–116. https://doi.org/10.1006/exer.1997.0419
12. Aoki S, Makino J, Nagashima A, Takezawa T, Nomoto N, Uchihashi K, Matsunobu A, Sanai T, Sugihara H, Toda S (2011) Fluid flow stress affects peritoneal cell kinetics: possible pathogenesis of peritoneal fibrosis. Perit Dial Int 31(4):466–476
13. Jester JV, Barry-Lane PA, Cavanagh HD, Petroll WM (1996) Induction of alpha-smooth muscle actin expression and myofibroblast transformation in cultured corneal keratocytes. Cornea 15(5):505–516
14. Jester JV, Petroll WM, Cavanagh HD (1999) Corneal stromal wound healing in refractive surgery: the role of myofibroblasts. Prog Retin Eye Res 18(3):311–356
15. Kawakita T, Espana EM, He H, Li W, Liu CY, Tseng SC (2005) Intrastromal invasion by limbal epithelial cells is mediated by epithelial-mesenchymal transition activated by air exposure. Am J Pathol 167(2):381–393. https://doi.org/10.1016/S0002-9440(10)62983-5
16. Netto MV, Mohan RR, Sinha S, Sharma A, Dupps W, Wilson SE (2006) Stromal haze, myofibroblasts, and surface irregularity after PRK. Exp Eye Res 82(5):788–797
17. Verjans GM, Remeijer L, Mooy CM, Osterhaus AD (2000) Herpes simplex virus–specific T cells infiltrate the cornea of patients with herpetic stromal keratitis: no evidence for autoreactive T cells. Invest Ophthalmol Vis Sci 41(9):2607–2612
18. Wang Z, Yang H, Tachado SD, Capó-Aponte JE, Bildin VN, Koziel H, Reinach PS (2006) Phosphatase-mediated crosstalk control of ERK and p38 MAPK signaling in corneal epithelial cells. Invest Ophthalmol Vis Sci 47(12):5267–5275
19. Dewey C, Bussolari S, Gimbrone M, Davies PF (1981) The dynamic response of vascular endothelial cells to fluid shear stress. J Biomech Eng 103(3):177–185
20. Davies PF (2009) Hemodynamic shear stress and the endothelium in cardiovascular pathophysiology. Nat Rev Cardiol 6(1):16
21. Ahsan T, Nerem RM (2010) Fluid shear stress promotes an endothelial-like phenotype during the early differentiation of embryonic stem cells. Tissue Eng A 16(11):3547–3553
22. Akutagawa T, Aoki S, Yamamoto-Rikitake M, Iwakiri R, Fujimoto K, Toda S (2018) Cancer–adipose tissue interaction and fluid flow synergistically modulate cell kinetics, HER2 expression, and trastuzumab efficacy in gastric cancer. Gastric Cancer 21(6):946–955
23. Ren H, Wilson G (1997) The effect of a shear force on the cell shedding rate of the corneal epithelium. Acta Ophthalmol Scand 75(4):383–387
24. Molladavoodi S, Robichaud M, Wulff D, Gorbet M (2017) Corneal epithelial cells exposed to shear stress show altered cytoskeleton and migratory behaviour. PLoS One 12(6):e0178981
25. Kaji Y, Oshika T, Usui T, Sakakibara J (2005) Effect of shear stress on attachment of corneal endothelial cells in association with corneal endothelial cell loss after laser iridotomy. Cornea 24(8):S55–S58
26. Yamamoto Y, Uno T, Joko T, Shiraishi A, Ohashi Y (2010) Effect of anterior chamber depth on shear stress exerted on corneal endothelial cells by altered aqueous flow after laser iridotomy. Invest Ophthalmol Vis Sci 51(4):1956–1964
27. Aoki S, Toda S, Ando T, Sugihara H (2004) Bone marrow stromal cells, preadipocytes, and dermal fibroblasts promote epidermal regeneration in their distinctive fashions. Mol Biol Cell 15(10):4647–4657
28. Sugihara H, Toda S, Miyabara S, Kusaba Y, Minami Y (1991) Reconstruction of the skin in three-dimensional collagen gel matrix culture. In Vitro Cell Dev Biol 27(2):142–146
29. Inoue T, Toda S, Narisawa Y, Sugihara H (2001) Subcutaneous adipocytes promote the differentiation of squamous cell carcinoma cell line (DJM-1) in collagen gel matrix culture. J Investig Dermatol 117(2):244–250
30. Ootani A, Li X, Sangiorgi E, Ho QT, Ueno H, Toda S, Sugihara H, Fujimoto K, Weissman IL, Capecchi MR (2009) Sustained in vitro intestinal epithelial culture within a Wnt-dependent stem cell niche. Nat Med 15(6):701
31. Wilson SE, Netto M, Ambrosio R Jr (2003) Corneal cells: chatty in development, homeostasis, wound healing, and disease. Am J Ophthalmol 136(3):530–536
32. Kalluri R, Zeisberg M (2006) Fibroblasts in cancer. Nat Rev Cancer 6(5):392–401. https://doi.org/10.1038/nrc1877
33. Khubutiya MS, Vagabov AV, Temnov AA, Sklifas AN (2014) Paracrine mechanisms of proliferative, anti-apoptotic and anti-inflammatory effects of mesenchymal stromal cells in models of acute organ injury. Cytotherapy 16(5):579–585. https://doi.org/10.1016/j.jcyt.2013.07.017
34. Dittmer J, Leyh B (2014) Paracrine effects of stem cells in wound healing and cancer progression. Int J Oncol 44(6):1789–1798
35. Bowling B (2015) Kanski's clinical ophthalmology, 8th edn. Elsevier Health Sciences, London
36. Myrna KE, Pot SA, Murphy CJ (2009) Meet the corneal myofibroblast: the role of myofibroblast transformation in corneal wound healing and pathology. Vet Ophthalmol 12:25–27
37. Wilson SE (2012) Corneal myofibroblast biology and pathobiology: generation, persistence, and transparency. Exp Eye Res 99:78–88
38. Kawashima M, Kawakita T, Higa K, Satake Y, Omoto M, Tsubota K, Shimmura S, Shimazaki J (2010) Subepithelial corneal fibrosis partially due to epithelial-mesenchymal transition of ocular surface epithelium. Mol Vis 16:2727
39. Furukawa F, Matsuzaki K, Mori S, Tahashi Y, Yoshida K, Sugano Y, Yamagata H, Matsushita M, Seki T, Inagaki Y (2003) p38 MAPK mediates fibrogenic signal through Smad3 phosphorylation in rat myofibroblasts. Hepatology 38(4):879–889
40. Caraci F, Gili E, Calafiore M, Failla M, La Rosa C, Crimi N, Sortino MA, Nicoletti F, Copani A, Vancheri C (2008) TGF-β1 targets the GSK-3β/β-catenin pathway via ERK activation in the transition of human lung fibroblasts into myofibroblasts. Pharmacol Res 57(4):274–282

Publisher's note Springer Nature remains neutral with regard to jurisdictional claims in published maps and institutional affiliations.